Modelling and Analysis of Particle and Pore Structures in Soils

Tobias Mehlhorn[1], Steffen Prohaska[2], Ulrike Homberg[2] and Volker Slowik[1]

[1] Hochschule für Technik, Wirtschaft und Kultur Leipzig (FH)
mehlhorn|slowik@fbb.htwk-leipzig.de
[2] Zuse Institute Berlin (ZIB) prohaska|homberg@zib.de

Summary. This work presents a numerical model of an idealised grain structure consisting of spheres and a method to derive the geometric characterization of the corresponding pore space. Two different starting points exist for obtaining the pore structure. Real grain structures can be obtained via computed tomography followed by image processing. Idealised grain structures, consisting of spheres, can be numerically modelled. In this paper we first concentrate on modelling, then we present a definition of pore space usable for idealised structures, but also extensible to real grain structures.

Key words: pore, pore throat, modelling

1 Introduction

Suffosion is the transport of fine grain through the pore space of the coarse grain, caused by water flow. Initially the matrix of the carrier structure stays immobile, while the mobile grain is washed out of the soil. The density of the soil declines and, eventually, the stability of the soil can suddenly decrease, causing, for example, failure of embankments.

The possibility of suffosion depends on the geometry of the grains and their pore structure. The geometry must be such that mobile grains can move through the pore space. In particular, soils with a gap grading are at risk. The geometric possibility alone, however, does not mean that suffosion necessarily occurs. Hydrodynamic criteria must be met too. But without the geometric possibility suffosion is never possible. Thus, understanding the geometric situation in soil is crucial for understanding suffosion.

The geometry of the real grain and pore structure in soils is not easily accessible. While it is relatively easy to measure the distribution of particle sizes by sieving, the geometric organization of the particles cannot be revealed in this way.

Computed tomography (CT) can provide three-dimensional images of the soil structure. CT, however, is quite expensive and thus the number of specimens that can be analysed is limited; and CT is only the first step towards determining the geometric situation. In

addition, image processing is required, which typically requires further work, like adjusting processing parameters to the particular specimen.

Modelling the grain and pore structure can be an alternative to examining real soils and modelling can provide geometric parameters available for an idealised situation that are hard to derive in real soils. Given the distribution of particle sizes, a model can provide, for example, a geometric description of the pore space suitable for analysing the possibility of particle transport by percolation theory. Further parameters can also be derived. Enzmann [3], for example, describes "the computermodell PoreFlow [...] that computes the effective hydraulic properties from the microscopic flow and transport through pore space".

We present a model of an idealised grain structure consisting of spheres and a method to derive the geometric characterization of the corresponding pore space. The model of grain structure is created by means of an algorithm using a combined formulation of geometric gravity based criteria and a stochastic-heuristic approach. The pore space is described as a graph whose edges connect the pores and store the diameter of the largest particle that can move along this edge. We further describe how the pore graph can be computed analytically and how it can be approximated by discrete geometry. This work is part of an approach to derive a new geometric suffosion criteria. This is described in [11].

2 Modelling of the Grain Structure

The algorithm for generating the model allows a systematic variation of particle size distribution as well as of particle content. Models created in this way are analysed regarding to the pore structure. Certain criteria the model needs to satisfy are essential. Those are defined as follows: All particles have to be stable. That means there are at least three points the particle lies on and the projection of its centers of gravity has to be inside the polygon whose vertices are the contact points. The particles must not overlap each other and the bounding box of the modelled volume. Furthermore, the predefined particle size distribution and packing density C has to be achieved

$$C = \frac{\sum particle\ volumes}{specimen\ volume} \tag{1}$$

2.1 Particle Structure

Particles are created in fractions of a grading curve and every particle's radius is defined at random within the limits of that fraction. Our approach allows an accurate reproduction of grading curves in comparatively short calculating time.

Our algorithm works as follows: After creating the particles complying with given parameters, the largest fraction is allocated first. Here, according to the stochastic-heuristic approach, a position within the specimen body is randomly selected. Subsequently, starting from that position a search for possible "neighbours" is performed. This search is restricted to an area under the starting position with twice the radius of the largest particle in the grain-size distribution. Within that area, all possible stable positions for that particle are located and afterwards one from those positions is selected by chance. In case there is no position found meeting these criteria of location, a new starting position as well as a new searchable area

will be defined and tested. This process is repeated until the particle can be allocated or a maximum number of trials is reached. Criteria applying to this are a stable location as well as no overlapping with other particles or the specimen boundaries. To latter, however, the particles can have contact with. Spheres which can not be allocated are deleted from the grain-size distribution. Figure 1 shows a grain structure created using this algorithm.

2.2 Carrier Structure

The carrier structure consists only of immobile particles. Immobile particles are the ones having four contact points minimum. At least one of these points has to be on the opposite side of the plane formed by the other contact points and shifted to the particle center. Then, kinematic constraint is ensured. Detaching the carrier structure from the particle structure is necessary when using parts of realistic grain-size distributions having a ratio of

$$k = \frac{R_{max}}{R_{min}} \geq 4,449 \tag{2}$$

according to which, following Ben Ʌim and Le Goff [6], small spheres might be locked into pores. However, as these are not required for the stability of the structure, they have to be erased before further considerations.

For identifying the carrier structure, all particles are analysed concerning their position. The particles having a stable position only, but are not immobile, are deleted as these are potentially mobile, i.e. they might be able to move inside the structure or at least inside a pore space. Since the carrier structure is decisive for further examinations, especially for the assessment of the suffosion risk, these particles have to be removed. The carrier structure created in this way may now be used to characterize the pore structure as described in the following.

Figure 2 shows the carrier structure created out of the grain structure from Figure 1.

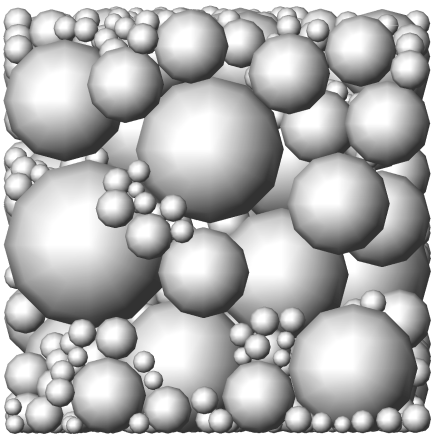

Fig. 1. Grain Structure

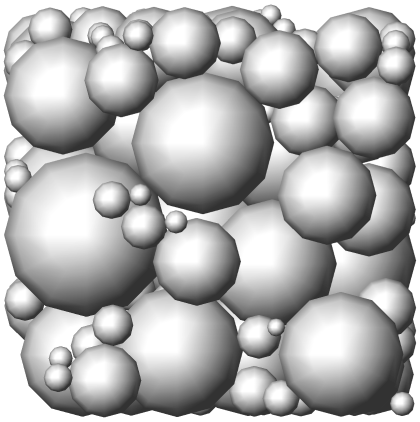

Fig. 2. Carrier Structure

3 Analysing Pore Space

The objective is to determine which particles can move within the pore space inside the carrier structure consisting of spheres. Small particles might freely move through the structure, while larger particles might be blocked at pore throats. Knowing the size of the largest particle that can move through a pore throat is crucial for analysing the possibility of particle transport.

Analysing the distance to the surface of the grain is our basis for understanding possible particle transport. Particles must fit in the pore space. Thus, assuming spherical particles, their radii must be smaller than the distance to the nearest surface of all grains. At pore throats, we want to find the largest sphere that can pass through the throat. Such a sphere can touch several grains but must not intersect with any of them.

Bisectors and the medial axis provide a mathematical framework for analysing the distance to the grain structure. The bisector of two objects O_1 and O_2 in $\mathbb{R}^3$ is defined as the set of all points that have equal distance to both objects [7]. A bisector in three-dimensional space is a surface that lies centrally between the two objects. If the objects cannot be distinguished, the symmetry set replaces the bisector: The symmetry set of a single solid object O is defined as the centers of spheres that touch O in two or more points. By restricting the eligible spheres, the medial axis can be defined: The medial axis is defined as the centers of spheres that touch O in two or more *closest* points, that is there is no point of O closer to the center of the sphere than the touching points. From the large amount of publications that discuss the medial axis, we only mention a few of them here. Originally, the medial axis was introduced by Blum [2]. A recent review of the state of the art of computing the medial axis is given by Attali et al. [1]. Giblin et al. [4] classify the medial axis into five types of points, which are organized into sheets, curves, and points.

We capture the essential information about the pore space in the pore graph. The vertices of the pore graph describe the pore centers and its edges describe possible paths to neighboring pores. The size of the largest particle that can freely move between two pores is associated with the edge connecting the two pores. As Giblin et al. [4] discuss, the centers of spheres that touch O in three or more closest points form a one-dimensional subset of the medial axis, which can be interpreted as a graph. This is nearly what we are looking for. In contrast, however, to a single object that is the basis for the definition of the medial axis, our grain structure is given as distinct objects, so we can incorporate this knowledge in the description of the pore graph. Assuming a collection of n grains $O_1, \ldots, O_n$, the pore graph is defined as the set of points that have equal smallest distance to three or more grains O_i. Points that have equal smallest distance to four grains are the vertices of the graph. They are connected by edges consisting of points that have equal smallest distance to three grains.

3.1 Computing the Pore Graph Analytically

The pore graph contains the smallest diameter along the edges connecting two pores which is the pore throat. These pore throats are described by their location and radius. To define the pore graph points, graph intersections as well as their length is given. Here, graph points are those points lying on the graph and in equal distance from three or more spheres being assinged to the graph. The pore itself is described by its volume, the diameter of the largest sphere fitting in the pore space and the number of pore throats.

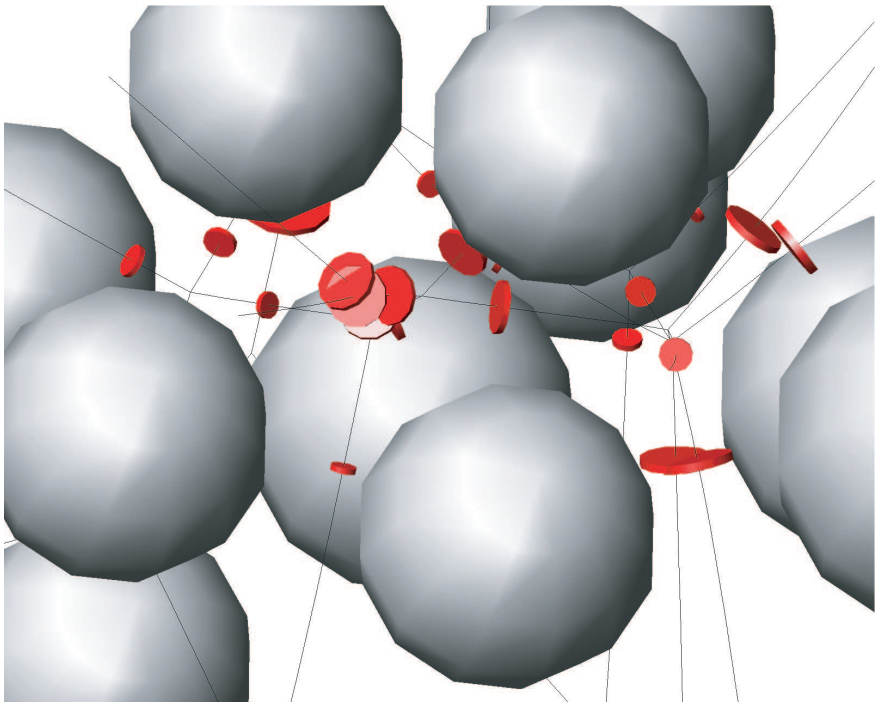

Fig. 3. A pore graph obtained analytically. The circles are the pore throat. The spheres are scaled to 75% and the circels to 40% of their original size in order to open the view to the otherwise occluded inner pores.

A throat in general can also be described as the utmost circle contacting three starting spheres, and lying in the plane through these three starting sphere's centers if no other sphere is intersected. These throats are the starting point to a description of pore space. Graph points are calculated by expanding the starting spheres stepwise by throat radius and ΔR as intersections of the so enlarged starting spheres. To create the pore graph plane two graph points and the throat center are cited, since all graph points lie inside a plane perpendicular to the starting points centers' plane. That graph plane is now intersected with the dilated starting points of the neighbour throat, from which a possible graph intersection as well as the appropriate distance to the starting spheres may result. Both, intersections and distance are assigned to every particular pore graph and form the boundary in creating graph points. Figure 3 depicts the pore graph computed analytically.

That way of approaching determining pore graphs has the advantage to be able to create curved graphs and so make a description of the pore space for a larger k-ratio possible as well.

3.2 Computing the Pore Graph using Discrete Geometry

Discrete geometry provides an alternative way of computing the pore graph. We directly mimic the definition of the pore graph, as the set of points that have equal smallest distance to three or more grains O_i, by well-known image processing algorithms: 1) The grains are scan-converted, that is they are sampled onto a regular grid of voxels. Each voxel is assigned

the identifier i of the grain O_i that covers this voxel. Background voxels, not covered by any grain, are assigned zero. 2) Next, the distance transformation of the grain structure is computed [5]. The result contains the distance to the nearest grain at each voxel. 3) The watershed transform [10] of the distance transform is now computed, using the scan-converted spheres as seeds. This results in a volume that is completely labeled with the grain identifiers. The label at each voxel identifies the nearest grain. 4) We identify voxel neighborhoods of size $2 \times 2 \times 2$ that contain three or more labels, because these are the neighborhoods that contain points that have equal distance to at least three grains. For each such neighborhood we mark a representative voxel (the bottom, left, front voxel) in the resulting volume. All other voxels of the result are marked as background. 5) The resulting (thick) voxel skeleton is post-processed by thinning [9] to remove thick parts. 6) The thin skeleton is converted to a graph, as described in [8]. In addition, the distance map is evaluated along the pore graph edges. Figure 4 depicts a visualisation of a pore graph computed in the described way.

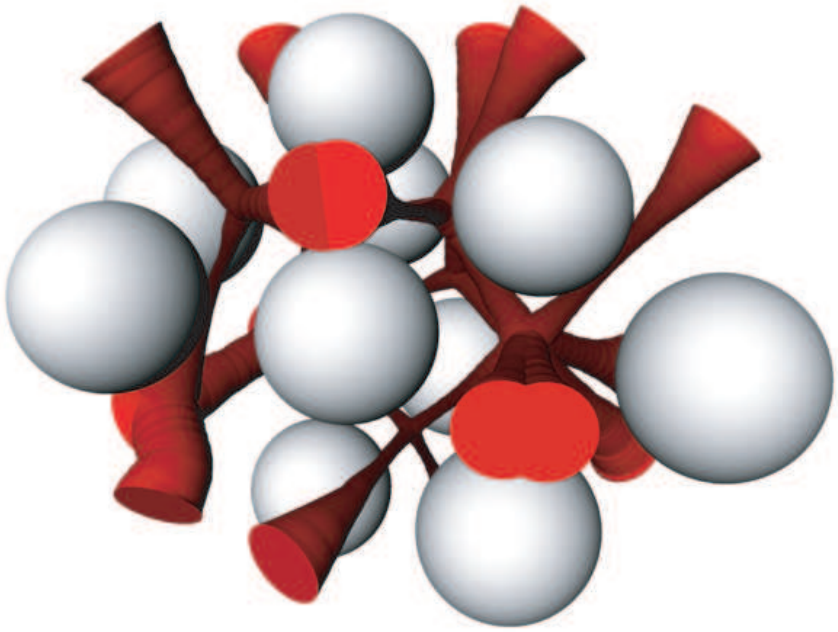

Fig. 4. A pore graph computed using discrete geometry. The pore graph is depicted in red. A high saturation emphasizes thicker parts. The spheres are scaled to 75% and the edges to 40% of their original radius in order to open the view to the otherwise occluded inner pores.

4 Results and Discussion

Modelling of suffosive soil is made possible by the here presented algorithm for creating grain structures consisting of spherical particles. All models were scrutinized concerning overlapping of spheres with each other or the specimen body. The localisations of all spheres were checked, thus all spheres lie stable at least. These tests were realized in cubic specimen bodies

having a size ratio of $2.5\,d_{max}$ to $5\,d_{max}$ and containing a maximum of 10^5 spheres which have diameters between $d_{min} = 0.00063\,m$ and $d_{max} = 0.02\,m$. We observed a dependence between specimen body size and the maximum grain, which, as expected, leads to an approach of the really arranged particle size distribution with the one determined before while undergoing a sinking ratio. It is to assume that at a specimen body size of about $10\,d_{max}$, a size commonly found in literature, the particle size distribution is reproduced exactly. The evidence of that is still to be provided as at the moment the computing time to create a system consisting of approximately 10^5 spheres and with a specimen body size of $5\,d_{max}$ takes approximately one day on a current desktop PC (single core, 3.0 MHz). Assuming that the algorithm shows an almost proportional dependence between number of spheres and computing time, a parallel implementation running on multi core processors could achieve the speed-up that make computing larger models feasible. Then it would be possible to scrutinize and evaluate systems having a size of $10\,d_{max}$ and consisting of about $4 \cdot 10^5$ spheres.

The algorithm deriving the carrier structure deletes all potentially mobile particles not being involved in building such a structure. If this algorithm is applied infinitely often to the system with a widely staged grain size distribution of a soil threatened by suffosion there is no convergence and all grains are deleted one by one. This might be caused by the algorithm itself or could be a first sign for a suffosion risk. This validation is subject of further work. Among other things, an application to a structure created following a grain size distribution of a soil not being at suffosion risk is desirable as well as a validation based upon the pore graph by putting the particular pore graphs of the single intermediate steps opposite each other. This validation is an important step on the way to a suffosion criterion.

As the carrier structure is used as base the deduction of the pore graph is possible. This provides the input parameters for the percolation theory. An extension of the presented algorithms for using ellipsoid particles and scaling to larger data sets are planned.

For synthetic grain structures consisting of spheres, analytic computations and discrete geometry yield comparable pore graphs. Both methods compute approximately the same pore graph and both methods compute an approximate distance along the edges, which can be used to derive the pore throat diameter.

For spherical grains, the analytic solution, however, yields better results than discrete geometry. The analytic solution is only limited by floating point precision, while discrete geometry, on the other hand, is limited by its discrete nature. The chosen voxel resolution limits approximation quality of the location and the distance to the grains. Although discretisation artifacts can somehow be removed by post-processing, for example smoothing the resulting skeleton, we cannot completely avoid them.

An advantage of discrete geometry is, though, that it naturally extends to objects of arbitrary shape. Arbitrary objects can be provided as labels in a voxel volume and the discrete method described can compute a pore graph. This will allow us to apply the method to grain structure segmented in image data of real soil specimens acquired by computed tomography.

We explicitly refer to individual grains in the definition of the pore graph and exploit this when computing the pore graph. Thus, individual grains must be provided as input to our algorithm. We could loosen this input requirement by referring to the medial axis, instead of bisectors. Individual grains would no longer be needed, avoiding the need for segmenting the grain structure into individual grains. A single large grain structure O would be sufficient input. But the watershed algorithm, which is part of our discrete method, could no longer

be used as is, because of lacking seeds. It is future work to investigate how our method could be modified to support a single large grain structure.

5 Conclusions

The creation of 3D particle packings is possible. The reduction of the packing to a carrier structure is a very promising approach and is base for analysing the pore space. The analyses using the presented techniques show good chances of success for idealised as well as for real structures. A further validation of the pore graphs in large systems is planned. As the knowledge about the pore graph is crucial for understanding suffosion, we expect that the work presented will contribute significantly to defining a suffosion criteria as outlined in [11].

6 Acknowledgement

The authors acknowledge the German Research Foundation (DFG) for supporting the research project "Conditions of suffusive erosion phenomena in soil". This work was also supported in part by the Federal Institute for Materials Research and Testing (BAM).

References

1. D. Attali, J. D. Boissonnat and H. Edelsbrunner. *Stability and computation of the medial axis – a state-of-the-art report.* In Möller, T., Hamann, B., and Russell, B., editors, Mathematical Foundations of Scientific Visualization, Computer Graphics, and Massive Data Exploration. Springer-Verlag, 2004.
2. Harry Blum. A transformation for extracting new descriptors of shape In *Models for the Perception of Speech and Visual Form*,pages 362–380. MIT Press, Cambridge, MA, 1967.
3. F. H. Enzmann. *Modellierung von Porenraumgeometrien und Transport in korngestützten porösen Medien.* PhD thesis, Johannes-Gutenberg-Universität Mainz, 2007.
4. P. Giblin and B. B. Kimia. *A formal classification of 3D medial axis points and their local geometry.* IEEE Trans. Pattern Analysis and Machine Intelligence, 26(2):238–251, 2004.
5. M. W. Jones, J. A. Baerentzen and M. Sramek *3D distance fields: A survey of techniques and applications.* IEEE Trans. Visualization and Computer Graphics, 12(4):581–599, 2006.
6. R. Ben Λim and P. Le Goff. Powder Technology 1:281-290, 1967.
7. Martin Peternell. Geometric Properties of Bisector Surfaces. In *Graphical Models*, 62(3):202–236, 2000.
8. S Prohaska *Skeleton-Based Visualization of Massive Voxel Objects with Network-Like Architecture.* PhD thesis, University of Potsdam, 2007.
9. C. Pudney *Distance-ordered homotopic thinning: A skeletonization algorithm for 3D digital images.* Computer Vision and Image Understanding, 72:404–413, 1998.
10. J. B. T. M. Roerdink and A. Meijster *The watershed transform: Definitions, algorithms and parallelization strategies.* Fundamenta Informaticae, 41(1-2):187–228, 2000.
11. O. Semar, R. Binner, U. Homberg, U. Kalbe, T. Mehlhorn, S. Prohaska, V. Slowik and K. J. Witt Conditions for Suffosive Erosion Phemomena in Soils – Concept and Approach –. In K. J. Witt, editor, *Proc. Work. Internal Erosion*, Weimar, 2008.